COLD TEST ON C-BAND STANDING-WAVE ACCELERATOR*

S. H. Kim[#], H. R. Yang, S. I. Moon, J. Jang, Y. M. Gil, M. Cho, and W. Namkung
Department of Physics, POSTECH, Pohang 790-784, Korea

S. J. Park and J. S. Oh
PAL, POSTECH, Pohang 790-784, Korea

Abstract

For a compact X-ray source, we designed a C-band standing-wave electron accelerator. It is capable of producing 4-MeV electron beams with 50-mA peak beam current. As an RF source, we use 5-GHz magnetron with duty factor of 0.08%. The accelerating structure is bi-periodic and on-axis coupled structure, operated with π/2-mode standing waves. Each cavity in the bunching and normal cell is designed by the MWS code and measured with aluminium prototype cavity. As per the dispersion relation derived from the measurement results, calibration factor obtained for the actual copper cavity.

INTRODUCTION

The electron accelerator is widely used for industrial applications, for example, a contraband detection, material processing, a medical diagnosis and therapy, sterilizing food, and environmental processing [1]. Environmental processing such as DeSOx or DeNOx and sterilization processing require an average beam power of several tens of kilowatts which depends on the processing speed. The contraband detection requires 5-10 MeV with the pulsed beam current of about 150 mA [2, 3].

We are developing an electron accelerator for an X-ray source. With pulsed 1.5-MW input RF power, it is producing 4 MeV at the 50-mA pulsed beam current. The beam energy can be varied from 3 to 6 MeV with input RF power of 1 to 5 MW. In this paper, we present design of overall accelerator system, including the accelerating structure. Also we present design details of accelerator cavity and measurement results of prototype cavity.

ACCELERATOR OVERVIEW

The accelerator uses a 5-GHz CPI magnetron as an RF source. It is capable of producing 1.5-MW RF with the 4-μs pulse length and the 200-Hz repetition rate. The WR187 waveguide network transports the RF power to the accelerating column. This waveguide is filled with atmospheric pressure SF_6 gas. The pulse modulator supplies the 40-kV and 90-A pulsed power to the magnetron with the 4-μs pulse length [4]. It also supplies the 20-kV pulsed voltage to an E-gun. The E-gun is a diode-type thermionic DC gun, capable of injecting a pulsed 150-mA beam.

The accelerating column is attached to the E-gun directly as shown in Figure 1. For the compact structure, a pre-buncher cavity with a drift tube is omitted. Furthermore, any solenoids magnet is not used since the beam current is low enough to be focused by the intrinsic focusing effect of the standing-wave electric field [5].

Table 1: The design parameters for the accelerator

Accelerator Parameters	
Operating Frequency	5 GHz
Input RF Power (pulsed)	1.5 MW
Pulse Length	4 μs
Repetition Rate	200 Hz
E-gun Voltage	20 kV
Input Beam Current (pulsed)	150 mA
Output Beam Energy	4 MeV
Output Beam Current (pulsed)	50 mA
Output Beam Power (average)	160 W
Loss Beam Power (average)	9.6 W
Type of Structure	Bi-periodic, On-axis coupled
Operating Mode	SW π/2 mode
Beam Aperture Diameter	10 mm
Average Accelerating Gradient	13.3 MV/m
Number of Cells	10
Inter-cell Coupling	6%
Quality Factor*	11000
Effective Shunt Impedance*	90 MΩ/m
Transit-time Factor*	0.81

*Values for normal cells.

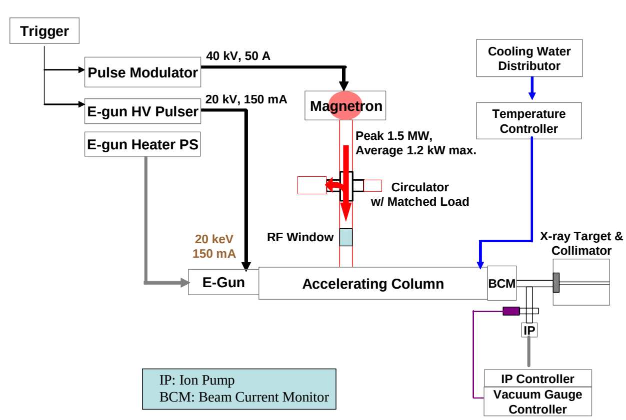

Figure 1: The block diagram of accelerator system.

*Work supported by PAL.
[#]khan777@postech.ac.kr

A bi-periodic and on-axis coupled structure is adopted for the π/2-mode standing-wave structure [6]. To increase the inter-cell coupling up to 6%, the magnetic coupling slot is bored on the wall between the accelerating cavity and the coupling cavity. The first three cells, in the Figure 2, are bunching cells with $\beta_{ph} = 0.7$. After bunching cells, the coupler cell is attached to the tapered C-band waveguide. All of the rest are normal cells with $\beta_{ph} = 1$.

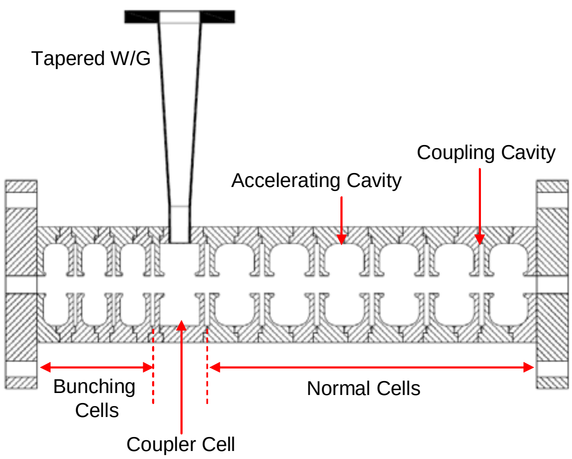

Figure 2: The cross-sectional view of the accelerating column. The magnetic inter-cell coupling holes are skewed to this plane.

CELL DESIGN AND PROTOTYPE TEST

For a bi-periodic accelerating structure, the dispersion relation is defined by

$$k^2 \cos^2 \varphi = [1 - (\omega_A^2 / \omega^2) + k_{AA} \cos 2\varphi] \times [1 - (\omega_C^2 / \omega^2) + k_{CC} \cos 2\varphi], \tag{1}$$

where ω is the resonance frequency of the coupled cavities at the φ mode, ω_A and ω_C are the resonance frequency of the accelerating cavity and the coupling cavity, and k is the coupling coefficient between the accelerating cavity to the nearest coupling cavity, while k_{AA} for two neighbouring accelerating cavities and k_{CC} for coupling cavities [7]. To excite the π/2-mode standing-wave with uniform field distributions, the π/2-mode chained resonant frequency should be the RF frequency for both the accelerating and coupling cavity.

A unit cell, composed of an accelerating cavity and a coupling cavity, is designed with the MWS code. To obtain ω_A, the boundary condition is used as shown in Figure 3. However, in case of the coupling cavity, the resonant frequency is different from ω_C by about 150 MHz when the mid-plane of the coupling cavity is shorted. The asymmetric field distribution in the coupling cavity makes this difference. To obtain ω_C, a detuned cavity boundary is used as shown in Figure 4. Since each end-cavity is detuned for the resonant frequency to be less than 3 GHz, the π/2-mode is excited only for the coupling cavity. With this boundary, the dispersion relation is consistent, as shown in Figure 5.

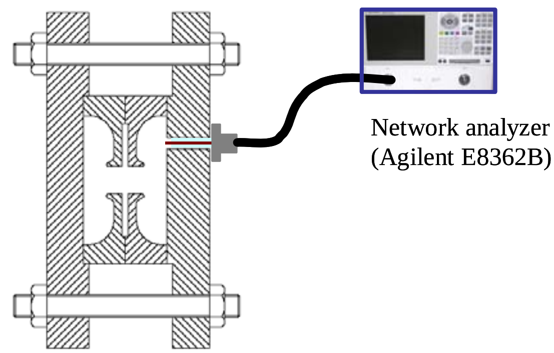

Figure 3: The experimental setup for measurement of the dispersion relation.

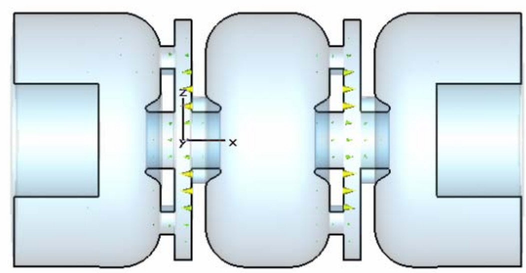

Figure 4: The detuned end-cavity boundary to excite the resonant frequency of the coupling cavity.

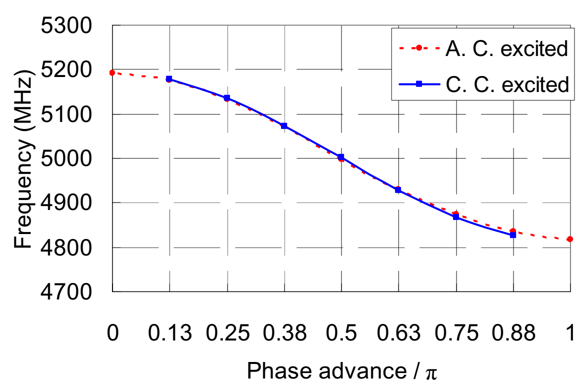

Figure 5: The dispersion relation under two different boundaries. One excites the accelerating cavity (dotted line) while the other excites the coupling cavity (straight line).

Prototype cavities were fabricated with aluminium. Measurement of ω_A is conducted with the setup in Figure 3. If more cells are added to this setup, the dispersion relation is obtained. From the dispersion relation, the stop-band can be calculated. According to measurement with a setup in Figure 3, ω_A is 4999.6 ± 0.163 MHz for the normal cell, and 5000.0 ± 0.661 MHz for the bunching cell. If cell numbers are increased, the π/2-mode resonant frequency for the accelerating cavity becomes lower, since k_{AA} is not definitely zero. The frequency is shifted by 2.75 MHz from the RF frequency, for the normal cell, as described in Table 2. The frequency shift is 6.72 MHz for the bunching cell. With these shifts, final dimension of the actual accelerating column will be determined.

Table 2: The measured frequencies of the π/2-mode

Cell Numbers	Bunching Cell (MHz)	Normal Cell (MHz)
1	5000.000	4999.600
2	4995.625	4998.500
3	4993.280	4997.875
4	-	4997.350
5	-	4997.250

For the dispersion relation, resonant frequencies are measured with 6 normal cells and 3 bunching cells, each. Fitting the measured values to Eq. 1, the dispersion relation is built up, as shown in Figure 6. For the normal cell, the π/2-mode frequency of the coupling cavity is estimated as 5000.2 MHz with a 6.1% inter-cell coupling constant. For the bunching cell, it is estimated as 5001.5 MHz with 7.5% coupling. The coupling cavity will be fabricated for the actual accelerating column by compensating above offset from the RF frequency.

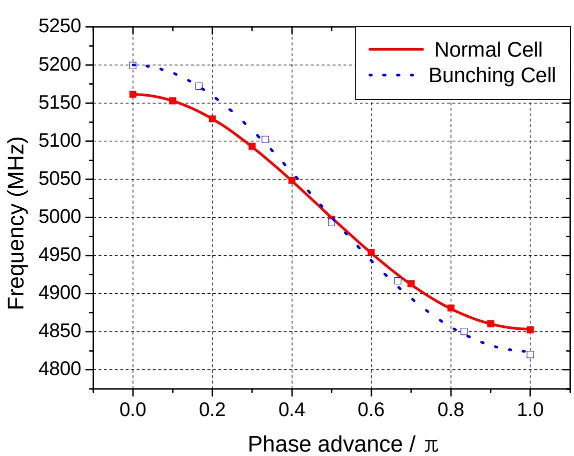

Figure 6: The dispersion relations of the normal and bunching cell.

CONCLUSION

Resonant frequencies are measured with the aluminium prototype cavity. The resonant frequency of the accelerating cavity is almost 5 GHz for both the normal and bunching cells. As the cell number is increased, the π/2-mode frequency becomes lower. This shift will be compensated for the actual cavity. The coupling cavity is designed with the detuned end-cavity boundary. As per the dispersion relation fitted by the measured frequencies, π/2-mode frequency of the coupling cavity is successfully close to the RF frequency.

The resonant frequency of the coupler cell and the external Q of the coupling hole are to be measured with the prototype cavity. Following this test, the bead test is to be conducted.

ACKNOWLEDGEMENT

The authors appreciate Prof. Luo Yingxiong at IHEP, Beijing for his advice on the accelerator system and the cavity design. They also appreciate PEFP group at KEARI, Korea for support to the simulation of the MWS code.

REFERENCES

[1] A. M. M. Todd, “Emerging Industrial Applications of Linacs,” in *Proc. of Intl. LINAC Conf.* (Chicago, IL, August 23-28, 1998), 1036 (1998).
[2] V. Pirozhenko, et al. “Complex for X-ray Inspection of Large Containers,” in *Proc. of EPAC 2006* (Edinburgh, Scotland, June 26-30, 2006), 2388 (2006).
[3] C. Hao, et al, “A New Type SW Linac Used in Industrial CT,” in *Proc. of APAC 2004* (Gyeongju, Korea, March 22-26, 2004), 429 (2004).
[4] S. D. Jang, Y. G. Son, J. S. Oh, Y. S. Bae, H. G. Lee, S. I. Moon, M. H. Cho and W. Namkung, J. Korean Phys. Soc. **49**, 309 (2006).
[5] L. Auditore, R. C. Barna, De Pasquale, A. Italiano, A. Trifiro, and M. Trimarchi, Phys. Rev. ST-AB **7**, 030101 (2004)
[6] H. Euteneuer, A. Jankowiak, M. Negrazus, and V. I. Shvedunov, “The 4.9 GHz Accelerating Structure for MAMI C,” in *Proc. of EPAC 2000* (Vienna, Austria, June 26-30, 2006), 1954 (2006).
[7] E. A. Knapp, B. C. Knapp, and J. M. Potter, Rev. Sci. Instr. **39**, 979 (1968).

